MNRAS **000**, 1–5 (2015) Preprint 14 July 2016 Compiled using MNRAS LATEX style file v3.0

Evidence for quasi-periodic oscillations in the optical polarization of the blazar PKS 2155–304

N. W. Pekeur[1⋆], A. R. Taylor[1,2], S. B. Potter[3] and R. C. Kraan-Korteweg[1]
[1] *Astrophysics, Cosmology and Gravity Centre, Department of Astronomy, University of Cape Town, Private Bag X3, Rondebosch 7701, SA*
[2] *Department of Physics and Astronomy, University of the Western Cape, Modderdam Road, Private Bag X17, Belville 7530, SA*
[3] *South African Astronomical Observatory, PO Box 9, Observatory 7935, Cape Town, SA*

arXiv:1607.03771v1 [astro-ph.HE] 13 Jul 2016

Last updated 2015 May 22; in original form 2013 September 5

ABSTRACT
Evidence for the presence of quasi-periodic oscillations (QPOs) in the optical polarization of the blazar PKS 2155–304, during a period of enhanced gamma-ray brightness, is presented. The periodogram of the polarized flux revealed the existence of a prominent peak at $T \sim 13$ min, detected at $> 99.7\%$ significance, and $T \sim 30$ min, which was nominally significant at $> 99\%$. This is the first evidence of QPOs in the polarization of an active galactic nucleus, potentially opening up a new avenue of studying this phenomenon.

Key words: galaxies: active – blazars: polarization – optical, blazars: individual: PKS 2155–304

1 INTRODUCTION

PKS 2155–304 is a blazar, a subclass of radio-loud active galactic nucleus (AGN) for which the relativistic jet is oriented close to the line-of-sight of the observer (Urry & Padovani 2009). Active galactic nuclei are powered by accretion of matter onto a $10^6 - 10^9 M_\odot$ supermassive black hole (SMBH). The observed emission is dominated by the jet and is characterized by intense and rapid brightness fluctuations across the electromagnetic spectrum, and the presence of polarization at optical to radio wavelengths. PKS 2155–304 exhibits significant variability on timescales ranging from minutes (HESS Collaboration 2007) to years (Fan & Lin 2000; Kastendieck, Ashley & Horns 2011). Short timescale variations, from minutes to hours, probe emission regions with sizes comparable to the gravitational radius of the central SMBH, while variations on timescales of months to years probe the jet structure. The timing signatures indicate that the emission is governed by correlated noise processes (Vaughan et al. 2003; Edelson & Nandra 1999; Vaughan 2005; Chatterjee et al. 2008, 2012; Kastendieck, Ashley & Horns 2011), possibly originating from instabilities in the accretion rate and jet.

Quasi-periodic variations have been reported for a small number of AGN. The clearest detection is a ~ 1 hour QPO in the $X-$ray light curve of the radio-quiet Seyfert galaxy RE J1034+396 (Gierliński et al. 2006). PKS 2155–304 is one of only a few blazars for which convincing evidence of quasi-periodic brightness variations have been documented. Long time-scale periodicities were discovered in the optical light curve of the source. Amplitude modulations with periods of 4 and 7 years (Fan & Lin 2000), and 315 days (Zhang et al. 2014; Sandrinelli et al. 2014) were identified, while a short time-scale oscillation of ∼4.6 hours was observed at $X-$ray energies (Lachowicz et al. 2009).

Evidence of quasi-periodic oscillations in the optical polarization of PKS 2155–304 is presented here. The polarization of the source was monitored from 25 – 27 July, 2009 with the HIgh Speed Photo-POlarimeter (HIPPO) of the Southern African Astronomical Society (SAAO). Gamma-ray observations were obtained independently with the High Energy Stereoscopic System (H.E.S.S.) over the same period, with indications of two $\gamma-$ray flares which bracket the occurrence of the optical polarization fluctuations. The acquisition of the optical polarization measurements and a description of the polarization and $\gamma-$ray observations is given in section 2. Section 3 presents an analysis of the observations. Discussion of the results follows in section 4, while the conclusions are presented in section 5.

2 OBSERVATIONS

The optical polarization of PKS 2155–304 was observed with the HIPPO (Potter et al. 2010), a rapidly rotating dual-channel photo-polarimeter operated by the SAAO. The instrument is mounted on the 1.9 metre Radcliffe telescope, which is located in Sutherland (South Africa). A comprehensive description of the polarimeter, data acquisition and reduction is presented in Potter et al. 2010. The most important instrument characteristics are described below.

⋆ Contact e-mail: nikki.pekeur@ast.uct.ac.za

© 2015 The Authors

Table 1. The mean daily optical polarization of PKS 2155–304 in July 2009.

MJD	$T_{\rm obs}$ (min)	p (%)	θ (°)
55037	290	3.7 ± 0.3	88 ± 2.5
55038	195	7.0 ± 0.3	67 ± 1.0
55039	197	8.3 ± 0.7	68 ± 0.5

The polarization of the incident light is measured by passing the incoming beam through a $\frac{1}{4}$ waveplate and a $\frac{1}{2}$ waveplate, which detects circular and linear polarization, respectively. The waveplates contra-rotate at 10 Hz, producing a modulation of the intensity dependent on the polarization of the beam. Simultaneous measurement of all Stokes parameters is obtained by rapidly sampling the polarization ellipse of the incoming beam as a function of angles during the rotation of the wave plates. A Thompson beam-splitter separates the beam into the orthogonal components of the electric field vector components, thereby allowing two independent measurements of the polarization. *UBVRI* colour filters, attached to each observation channel, enable two simultaneous colour measurements. Uncertainties in the calculated polarization are largely dependent on photon statistics, which is expected to be relatively small since PKS 2155–304 is a bright source ($m_B = 13^m.6$; Pica et al. 1988).

The intra-day variability (IDV) of the source was monitored from 25 – 27 July 2009 for a total of 9.23 hours using a time-resolution of 5 minutes. The linear and circular polarization of the source was recorded in the I– and B–band. A summary of the daily average of the polarization degree and the electric vector position angle (EVPA), or polarization angle[1], of the I– and B–band is presented in Table 1. The columns list the Modified Julian date (MJD), duration ($T_{\rm obs}$) and the polarization degree and polarization angle of the source. Table 1 demonstrates an increase in the polarization degree from approximately 4% to 8% between MJD = 55037 to 55038, accompanied by a decrease in the polarization angle from 88° to 68°. Historically, the polarization degree of PKS 2155–304 typically ranges from $2\% - 10\%$ on timescales of a few days (Tommasi et al. 2001), the EVPA displays a systematic decrease on timescales exceeding ten years (Dominici et al. 2008), which is consistent with our findings. Figure 1 illustrates the change in the polarization degree. The $\gamma-$ray light curve as recorded by the H.E.S.S. for photons with energies > 300 GeV, is superimposed. The increase in the fractional polarization is associated with an increase in $\gamma-$ray activity, with two prominent flares being detected in the $\gamma-$ray flux, I, (HESS Collaboration 2014). The first flare peaks at $I = (8.0 \pm 0.4) \times 10^{-11}$ ph cm^{-2} s^{-1} and is located at MJD = 55035. A subsequent rise is then seen in the $\gamma-$ray flux between MJD = 55038 and 55039, from $I = (1.9 \pm 0.4) \times 10^{-11}$ ph cm^{-2} s^{-1} to $I = (5.6 \pm 0.4) \times 10^{-11}$ ph cm^{-2} s^{-1}, which could be indicative of a developing flare. However, this cannot be verified due to a lack of observations past MJD = 55039. Note that the second rise in $\gamma-$ray flux is accompanied by a similar rise in the polarization degree by about one day.

[1] The polarization angle is measured from the North Celestial Pole towards the Celestial East.

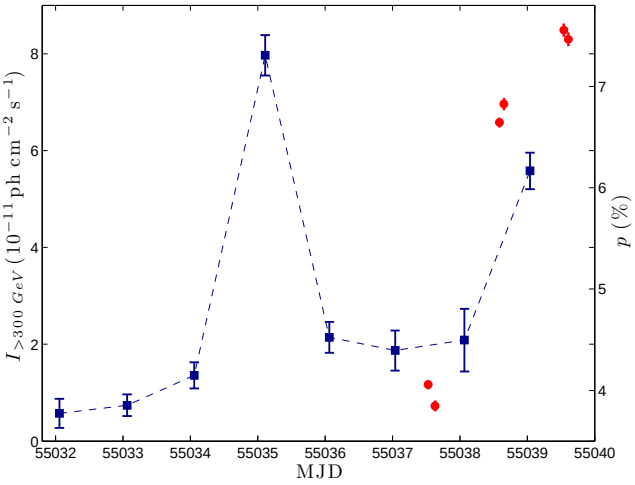

Figure 1. The $\gamma-$ray light curve of PKS 2155–304 for photons with energies > 300 GeV in July 2009, as seen by the H.E.S.S. (HESS Collaboration 2014). The $\gamma-$ray intensity I, measured in ph cm^{-2} s^{-1}, is represented by the filled circles. The I–band polarization degree p (%) is superposed on the $\gamma-$ray light curve and is symbolized by the filled red squares. Two prominent increases in the $\gamma-$ray flux are detected. The first peak occurs on MJD = 55035, at $I = (8.0 \pm 0.4) \times 10^{-11}$ ph cm^{-2} s^{-1}. Another increase in $\gamma-$ray flux, from $(1.9 \pm 0.4) \times 10^{-11}$ ph cm^{-2} s^{-1} to $(5.6 \pm 0.4) \times 10^{-11}$ ph cm^{-2} s^{-1} is seen between MJD = 55038 and 55039.

3 QUASI-PERIODIC OSCILLATIONS

The intra-day variations in the optical polarization was investigated by analyzing the high time resolution data taken over the course of each day. The number of photons collected in the I–band were typically an order of magnitude higher compared to the B–band. Since the measurement errors are dominated by photon statistics, the B–band observations display larger measurement errors. More robust measurements were recorded in the I–band, which is what we use in the following analysis.

Inspection of the IDV on MJD = 55037 over the 290 minutes of continuous observation (see Fig. 2) suggests that the amplitude of the polarization degree is modulated on a timescale of ~ 30 min. These short-term amplitude modulations are superposed on a slowly decreasing baseline. The oscillations thus precede the onset of the increase in the optical polarization degree seen in Fig. 1. It is noteworthy such short-term modulations are not seen on MJD = 55038 and 55039, after the onset of the rise in the polarized intensity and the second $\gamma-$ray flare.

To test for the presence of periodic components in the optical polarization we computed the periodogram, which measures the amount of variability power as a function of temporal frequency, normalized to the mean of the light curve, in units of (rms/mean)^2 per Hz (Schuster 1898; Vaughan 2005). The periodogram was oversampled by a factor of 10 relative to the grid defined by the Fourier frequencies $\nu_k = k/N\Delta T$ to provide good sampling of the spectrum, where N is the number of observations and ΔT is the sampling interval. The periodogram of the Stokes Q and U polarized intensities is displayed in Fig. 3. Two prominent peaks are detected at 565 ± 7 μHz and 1293 ± 6

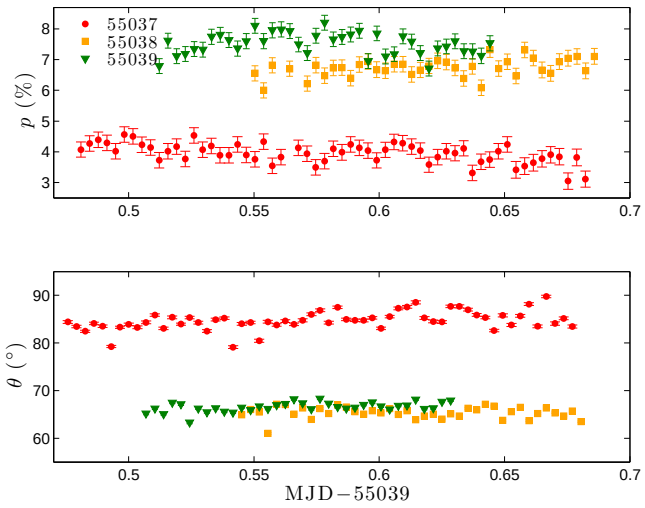

Figure 2. The intra-day variability of the I–band polarization (binned to 5 min) of PKS 2155–304 on MJD = 55037 (circles), 55038 (square markers) and 55039 (triangles). The top panel displays the polarization degree p (%), while the position angle of the electric vector θ (°) is shown in the bottom panel. The polarization degree appears to modulated by a periodic component on MJD = 55037.

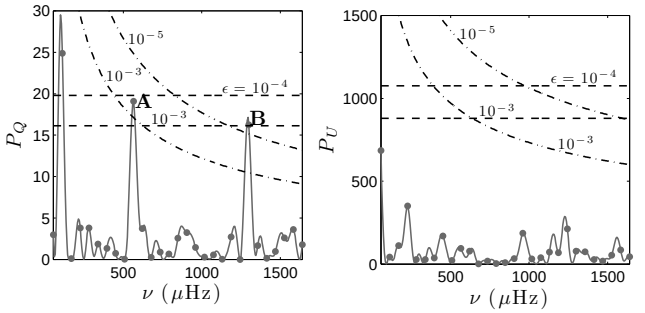

Figure 3. The periodogram of the polarized flux, in units of (rms/mean)^2 per Hz. The periodogram of the Stokes Q flux, P_Q, is presented in the left panel, while the periodogram of the Stokes U flux, P_U, is shown on the right. The filled circles represent the periodogram ordinates at the Fourier frequencies. Two prominent peaks are detected at $\nu_A = 565 \pm 7$ μHz and $\nu_B = 1293 \pm 6$ μHz, which are labelled as **A** and **B**, respectively. The false alarm probabilities for white noise, indicated by the dashed lines, and red noise, indicated by the dotted-dashed lines, are superposed.

μHz, labelled as A and B, respectively. Each peak signal is well-described by a Gaussian function, for which the uncertainty in the position of the peak is given by $\sigma_{\nu_0} = \mathrm{FWHM}/\left(2\sqrt{2\ln 2} \times \sqrt{snr}\right)$ (Condon 1997), where FWHM is the full-width half-maximum of the peak and snr is its signal-to-noise ratio. The period corresponding to peak A is $T = 29.4$ min and $T = 12.9$ for peak B. No dominant peaks are detected in the Stokes U periodogram. The lack of detection in U is consistent with a variation in polarized intensity (as opposed to angle), as the observed polarization position angle $\theta \approx 90°$ (see Table 1 and Fig. 2), places virtually all the polarized emission in Q.

Figure 4 displays the Stokes Q light curve folded to

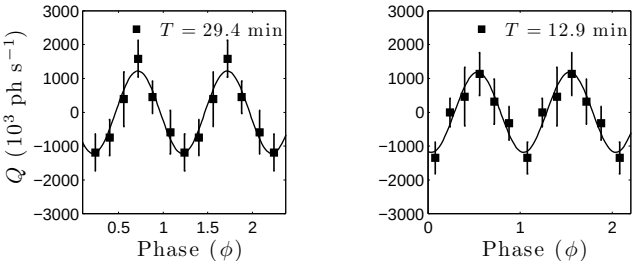

Figure 4. The Stokes Q light curve folded to $T = 29.4$ min and $T = 12.9$ min, averaged into six phase bins. Two cycles are plotted for clarity. A cyclic trend appears to be present for both trial periods. The solid line represents the best-fit sinusoid for each case.

the $T = 29.4$ min, the period of spectral component **A** and $T = 12.9$ min, the period of spectral component **B**. Two cycles are plotted for clarity. Although the amplitude modulation is small, a cyclic trend appears to be present for both periods. A non-linear least-squares fit to the data yields a best-fit sinusoid that agrees well with the phase-folded diagram, with a period of $T = 29.5$ min for signal A and $T = 12.9$ min for signal B.

The statistical significance of the periodogram was determined by comparing the observed peak power to the probabilities of deflections arising from a noise continuum $S = N\nu^{-\alpha}$ (or red noise), where α is the spectral index, or slope, and N is the flux normalization of the spectrum. The model spectrum is obtained by fitting a power-law to the observed periodogram using the least-squares (LS) method described in Vaughan 2005. The result of the fit is displayed in Fig. 5, which shows the Stokes Q power spectrum on a logarithmic axes. The slope is consistent with white noise ($\alpha = 0$), but a formal fit to the spectrum yields a de-biased best-fit line with $\alpha = 0.59 \pm 0.3$ (represented by the solid line). If S represents the true power spectral density, then the ratio $\gamma = 2P/S$ is scattered as a χ^2_2– distribution with two degrees of freedom and we can define confidence limits for the noise. The upper 99% confidence limit of the underlying continuum was calculated. Fig. 5 shows that the observed peaks are detected above the 99% confidence limit (represented by the red dashed line), with the chance probability of detecting peak A $\Pr[\gamma > \gamma_\epsilon] = 3.1 \times 10^{-4}$ (corresponding to $\sim 3\sigma$) and 3.4×10^{-6} for peak B, given the number of frequencies that were examined. The false alarm probabilities for the power-law model, and for white noise, are superposed on the periodogram in Fig. 3. The figure illustrates that the observed peaks exceed the $\epsilon = 10^{-3}$ false alarm threshold of white noise.

The robustness of this result was verified by generating 10^4 random light curves with the same mean, variance and sampling rate as the observations, following the procedure described in Timmer & König 1995. The resulting distribution of power for an underlying continuum with $\alpha = 0.6$ (the best-fit slope to the data) was recorded and the 99% and 99.7% confidence levels computed. The 99% confidence level from the simulated distribution is indicated by the teal dotted-dashed line in Fig. 5. Although the simulation shows that the LS test overestimates the significance of the periodic signal, peak A and peak B remain statistically significant,

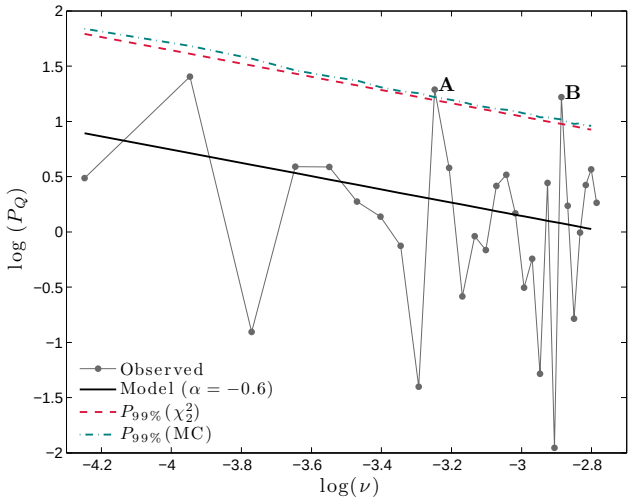

Figure 5. The power spectrum of the Stokes Q intensity, normalized to (rms/mean)^2 per Hz. The solid line represents the best-fit power-law with a slope $\alpha = 0.59 \pm 0.3$. The 99% confidence limit of the noise is represented by the dashed line. The robustness of this result was tested by generating 10^4 random light curves with the same mean, variance and sampling rate as the observations from an underlying continuum with $\alpha = 0.6$. The 99% confidence limit of the simulated power distribution is indicated by the teal dotted-dashed line.

with peak A detected at $> 99\%$ significance, while peak B is detected at $> 99.7\%$ significance.

To conclude, the periodogram of the polarized flux is consistent with the presence of a periodic component at $T \sim 13$ min, with $> 99.7\%$ significance, and $T \sim 30$ min, which was found to be nominally significant at $> 99\%$.

4 DISCUSSION

The optical emission in blazars is dominated by synchrotron radiation from relativistic electrons being accelerated in the jet's magnetic field. The polarization is determined by the degree of order and direction of the magnetic field, and the viewing angle of the observer. Since radiation from the jet is highly Doppler boosted, even for small changes in the viewing angle, significant brightness variations will be observed. Fast variations, such as those observed in the optical polarization of PKS 2155–304, therefore most likely originate in the Doppler boosted jet, from an emission region with a size which is comparable to the gravitational radius of the central engine. Using the timescale of the fastest periodic component as the variability timescale $t_{\rm var} \approx 13$ min, a redshift $z = 0.116$ (Falomo, Pesce & Treves 1993) and a Doppler factor $\delta \approx 30$ (Katarzynski 2008), yields an upper limit to the size of the emission region $R \lesssim c\delta t_{\rm var}/(1+z) \approx 10^{15}$ cm.

Quasi-periodic variations can arise if an emission feature with physical properties distinct from the ambient jet medium, such as a relativistic shock, propagates down a jet which contains quasi-helical structures, either in the magnetic field or electron density (e.g., Qian et al. 1991; Romero 1995). A relativistic shock propagating down such an inhomogeneous jet will result in successive peaks in the amplitude of the total and polarized emission at the viewing angle that provides the maximum boosting for the observer (e.g., Camenzind & Krockenberger 1992; Gopal-Krishna & Wiita 1992).

Turbulence behind the shock can also explain the presence of short-lived QPOs (Marscher et al. 1992). For such turbulent flows, the largest eddies will dominate the variability and the period of the period will be determined by their turnover times. The presence of one or more such turbulent cells behind the same shock also provides a possible explanation for the presence of multiple QPOs in the same signal.

5 CONCLUSIONS

Monitoring of the intra-day optical polarization of PKS 2155–304 revealed the first evidence for quasi-periodic oscillations in the polarized flux of an AGN. The periodogram showed the existence of a periodic component at $T \sim 13$ min, detected at $> 99.7\%$ significance, and $T \sim 30$ min, which was found to be nominally significant at $> 99\%$. The period of these oscillations are similar to the $T \approx 15$ min QPO seen in the optical light curve of the blazar S5 0716+714 (Rani et al. 2010), which provides further support for the existence of such short timescale periodicities in these sources.

Gamma-ray observations of the source over the same period showed that it was in a high state of activity, experiencing two $\gamma-$ray flares at very high energies (VHE, photons with energies exceeding a few GeV). The first simultaneous optical polarization measurements of the source during a high-state was recorded for the latter flare. Although the physical cause of this QPO is unclear, comparison with the VHE light curve showed that PKS 2155–304 experienced a $\gamma-$ray flare two days before the appearance of the QPOs and another peak two days later. The oscillations could therefore be related either to the late phase of post flare activity of the first flare, which is supported by the decreasing trend observed over the night (as opposed to increasing trend seen on the following nights, see Fig. 2) or due to transition between two different gamma-ray flares. Since blazar emission is dominated by synchrotron emission at low energies, which also leads to polarization, and inverse Compton emission at high energies, which both arise from the relativistic jet, this could suggest that the observed QPOs are part of a longer-lived phenomenon within the jet of PKS 2155–304.

ACKNOWLEDGEMENTS

The authors would like to thank the anonymous referee for many suggestions that significantly improved this paper.

We gratefully acknowledge the support of the South African National Research Foundation (NRF) and the Department of Science and Technology (DST) through the South African Square Kilometre Array Office. N.W.P. also thanks the Science Faculty at the University of Cape Town (UCT) and Centre for Space Physics at North-West University (NWU) for their support. The authors also thanks the H.E.S.S. Collaboration for taking the $\gamma-$ray observations, as well as Markus Böttcher for stimulating discussions.

REFERENCES

Aharonian F. et al., 2007, ApJ, 664, L71
Abramowski A. et al., 2014, A&A, 571, A39
Camenzind M., & Krockenberger M., 1992, å, 255,59
Chatterjee R. et al., 2008, ApJ, 689, 79
Chatterjee R. et al., 2012, ApJ, 749, 191
Condon J. J., 1997, PASP, 109, 166
Dominici T. et al., 2008, Proc. of the Workshop on Blazar Variability across the Electromagnetic Spectrum, Palaiseau, France, p. 35
Edelson R., Nandra K., 1999, ApJ, 514, 682
Falomo R., Pesce J. E., Treves A., 1993, ApJ, 411, L63
Fan J. H., Lin R. G., 2000, A&A, 355, 880
Gierliński M. et al., 2008, Nature, 455, 369
Gopal-Krishna, & Wiita P. J., 1992, å, 259, 109
Kastendieck M. A., Ashley M. C. B., Horns D., 2011, A&A, 123, 531
Katarzyński K. et al., 2008, MNRAS, 390, 371
Lachowicz P.et al., 2009, A&A, 506, L17
Marscher A. P., Gear W. K., Travis J. P, 1992, in Variability of Blazars, ed. E. Valtaoja & M. Valtonen, Cambridge: Cambridge Univ. Press, 85
Pica, A. J. et al., 1988, AJ, 96, 1215
Potter S. B. et al., 2010, MNRAS, 402, 1161
Qian S. J. et al., 1991, A&A, 241, 15
Rani B. et al., 2010, ApJ, 719, L153
Romero G. E., 1995, Ap&SS, 234, 49
Sandrinelli A., Covino S., Treves, A., 2014, ApJ, 793, L1
Schuster A., 1898, Terrestrial Magnetism, 3, 24
Timmer J., König M., 1995, A&A, 300, 707
Tommasi L. et al., 2001, ApJS, 132, 73
Urry C. M., Padovani P., 1995, PASP, 107, 803
Vaughan S., Edelson R., Warwick R. S., Uttley P., 2003, MNRAS, 345, 1271
Vaughan S., 2005, A&A, 431, 391
Zhang B. K., Zhao X. Y., Wang C. .X, Dai B. Z., 2014, Res. Astron. & Astrophys., 14, 933

This paper has been typeset from a TEX/LATEX file prepared by the author.